Regulating SQSTM1/P62 and Wnt/β-catenin signaling of EMT to constrain TNBC invasiveness.

Rajib Shome
Indian Institute of Technology Guwahati
Plaboni Sen
Indian Institute of Technology Guwahati
Siddhartha Sankar Ghosh (sghosh@iitg.ac.in)
Indian Institute of Technology Guwahati

Research Article

Keywords: EMT, MDR, Stemness, Wnt/β-catenin, SQSTM1/P62, siRNA, TNBC

Posted Date: May 16th, 2022

DOI: https://doi.org/10.21203/rs.3.rs-1630401/v1

Abstract

Purpose:

The prevalence of cells with mesenchymal features is one of the well-known characteristics of triple negative breast cancers (TNBCs); where cells have undergone epithelial to mesenchymal transition (EMT) and are found to be poorly differentiated, giving rise to cancer stem cells (CSCs). Wnt/β-catenin and Wnt/PCP signaling pathways are prominent contributor of EMT, stemness and CSC properties of TNBC. SQSTM1/P62 cooperates with the components of the Wnt/PCP signaling pathway and is critically involved at the interface of autophagy and EMT. Understanding these regulatory links proves to be an instrumental approach to prohibit progression of TNBC.

Methods:

siRNA targeting SQSTM1/P62 and inhibitor of Wnt/β-catenin (FH535) in conjunction was used to explore molecular modification of EMT and stemness markers. Flow cytometric assays reveled CSC and apoptotic population whereas migration and invasion assay assetred alteration of the metastatic property. Genes and proteins involved were studied at molecular level employing confocal microscopy, western blotting and qRT-PCR.

Results:

Although SQSTM1/P62 is not crucial for cell survival, cytotoxicity assay revealed synergistic interaction between the siRNA/inhibitor. Modulation of these important pathways helped in reduction of expression of genes and proteins contributing to CSC properties. Co-treatment reduced the colony formation and self-renewal properties. Furthermore, invasion assay revealed 5.22-fold downregulations of the metastatic property. Gene and protein expression analysis revealed the induction of EMT to MET. Moreover, co-treatment resulted in inactivation of non-canonical Wnt VANGL2-JNK signaling axis and depletion of p-AKT and p-STAT-3.

Conclusions:

The synergistic impact of inhibition of SQSTM1/P62 and Wnt/β-catenin signaling facilitates the development of a potential theraputic regimen for TNBC.

1 Introduction

Epithelial to mesenchymal transition (EMT) is a dynamic biological process that encompasses changes in the cellular organization by which epithelial cells lose their differentiated characteristics and instead gain mesenchymal features [1]. EMT induces cells to lose mechanical and physiological integrity of

tissues, develop mesenchymal features, exhibit accelerated invasion, and enhance resistance to apoptosis [1]. Although EMT is associated with normal developmental process, but it is rapidly establishing as one of the pivotal signaling mechanisms responsible for imparting the generation of invasive and metastatic characteristics to solid tumors. In addition to metastasis, EMT is also known to modulate the phenomenon of multi-drug resistance. Plenty of research has gradually revealed that the development of the EMT phenotype is interrelated and has a direct impact on drug resistance in breast cancer.

EMT, invasiveness, drug resistance, and metastasis are all important hallmarks of triple-negative breast cancer (TNBC), the most aggressive subtype of breast cancer that accounts for 15 to 20% of all occurrences [2]. Unlike other breast cancers, TNBCs lack expression of estrogen receptor (ER), progesterone receptor (PR) and human epidermal growth factor receptor 2 (HER-2), which renders them non-targetable and restricts to limited treatment options [3]. The occurrences of TNBC are predominantly associated with premenopausal women and the preponderance of mortality is attributed to metastasis and tumor recurrence. On account of the lack of effective targeted therapies, patients with metastatic TNBC (mTNBC) have a poor clinical prognosis, with a median overall survival (OS) time of roughly 13–16 months.

The prevalence of cells with mesenchymal features is one of TNBCs' well-known characteristics; where cells have undergone EMT and are found to be poorly differentiated. In fact, EMT is known to generate minimally differentiated cells which give birth to cancer stem cells (CSCs). CSCs have self-renewal potential and these cells can lead to different clonal populations, which results in intratumoral heterogeneity [4]. Intratumoral heterogeneity contributes to chemoresistance and subsequently tumor recurrence. Therefore, targeting CSCs may be an instrumental approach in treating EMT and CSC-rich TNBCs.

SQSTM1/P62 (Sequestosome-1; also known as p62) is a ubiquitin-binding scaffolding protein capable of functioning in diverse cellular processes [5]. SQSTM1/P62 predominantly participates in cell proliferation, survival, EMT, cell death signaling programs and autophagy regulation via its versatile protein adaptor functions [6]. This multi-domain protein interacts selectively with different signaling intermediaries, such as Raptor, Nrf2-binding site on Keap1, ubiquitin and LC3, to regulate metabolic reprogramming, antioxidant response and selective autophagy, respectively [6]. Multiple neoplasms, particularly breast cancer, have been shown to have aberrant SQSTM1/P62 overexpression. Furthermore, increased SQSTM1/P62 expression is linked to breast tumors with aggressive clinicopathological characteristics, such as overexpression of EGF receptor, HER-2, HER-3, and HER-4. Individuals with SQSTM1/P62 accumulation in triple-negative breast cancer had a greater chance of positive lymph node and lymphovascular invasion. Interestingly, experimental evidence suggests SQSTM1 mediated stabilization of the key EMT regulators and transcription factors [7]. These findings suggest that SQSTM1/P62 might be used as a therapeutic target for TNBC.

Numerous signaling pathways have been identified to be responsible for inducing and maintaining EMT and CSC characteristics. Among these signaling pathways, Wnt/β-catenin signaling has been reported to be a prominent contributor of EMT, stemness and CSC properties of TNBC. The Nuclear accumulation of β-catenin promotes EMT, cell motility, invasion, colony formation, stem cell-like properties, and chemoresistance [8]. Similarly, the Wnt/PCP (planar cell polarity) pathway regulates cancer cell motility and invasion and further cancer progression [9]. This, in turn, emphasizes a pivotal role of canonical and non-canonical Wnt signaling as one of the driving forces of TNBC tumorigenesis and metastasis. Recognizing the centrality of both canonical and non-canonical Wnt signaling in the molecular pathogenesis of TNBC via EMT and MDR, we postulated that modulating these pathways might be a method for achieving dramatic therapeutic results in TNBC. An intriguing correlation between Wnt signaling and SQSTM1/P62 is that SQSTM1/P62 cooperates with the components of the non-canonical Wnt/PCP signaling pathway and helps in EMT and oncogenesis [10].

Therefore, in the present study, we sought to investigate the impact of inhibiting canonical Wnt signaling and suppressing SQSTM1/P62 to further modulate the non-canonical Wnt/PCP pathway with an aim to influence EMT, MDR and stemness in TNBC cells. To inhibit Wnt/β-catenin signaling we have used small-molecule inhibitor FH535 which suppresses Wnt/β-catenin signaling [10]. Similarly, siRNA targeting human SQSTM1/P62 was used to silence the expression of SQSTM1/P62. Using monolayer culture and multicellular 3D spheroids we investigated the alteration in pathways and signaling cascades that govern the crosstalk between EMT, MDR, and stemness of TNBC, and the role of SQSTM1/P62 in that process.

2 Materials And Methods

2.1 Cell lines and culture conditions:

The human breast cancer cell lines MDA-MB-231 and MDA-MB-468 were purchased from the National Centre for Cell Science, Pune, India where it was tested and authenticated. Cells were cultured in Dulbecco's Modified Eagle's Medium-high glucose supplemented with L-glutamine, sodium pyruvate (Sigma-Aldrich, St. Louis, MI, USA), 10% fetal bovine serum (FBS) (Thermo Fisher Scientific, Waltham, MA, USA), Sodium bicarbonate (Sigma-Aldrich), 100 units/ml penicillin and 100 µg/ml streptomycin (Thermo Fisher Scientific). The cells were maintained in humidified air containing 5% CO_2 at 37°C. To induce EMT, cells were starved for 12 h in 0.5% serum medium and incubated in 20 nM EGF for 30 min prior to treatment.

2.2 siRNA transfection:

For siRNA transfection, reverse transfection was carried out with Lipofectamine™ RNAiMAX Transfection Reagent (Invitrogen, Carlsbad, CA, USA) according to the manufacturer's instructions. MISSION® esiRNA targeting human SQSTM1/P62 (Catalog No: EHU027651) and Universal Negative Control #1 (Catalog No: SIC001) was purchased from Sigma-Aldrich, St. Louis, MI, USA. While performing reverse transfection for SQSTM1/P62, all the other cells were transfected with the negative control siRNA using the same transfection protocol.

2.2 Cell viability and drug combination assays:

To detect the percentage of the viable cell following treatment, alamarBlue (Thermo Fisher Scientific) assay was performed in both monolayer culture and 3D spheroids. Upon entering into the live cells, the active ingredient of the alamarBlue resazurin is reduced to resorufin [11]. Following the treatment period, alamarBlue was added in 1X concentration for individual analysis and incubated at 37°C under 5% CO_2 humidified conditions for 2.5 h in case of monolayer culture and 4 h in case of spheroids. Afterward, absorbance values were recorded at 570 nm with a reference of 600 nm using a microplate reader (Infinite M200 Pro, Tecan, Switzerland). To determine the cell viability percentage, the following formula was used-

$$\text{CellViability}(\%) = \frac{(abs570 - abs600)\,Sample}{(abs570 - abs600)\,Control} x100$$

The sigmoidal-dose response curves were plotted using GraphPad software and the inhibitory concentration-50 (IC_{50}) values were determined. The effect of the combination was analyzed using Chou and Talalay combination index (CI) using Calcusyn software (Biosoft) [12].

2.3 Cell cycle analysis:

To detect the effect of the inhibition of the signaling pathway on cell cycle progression, flow cytometry-based cell cycle analysis was performed. Cells were seeded in 6 well tissue culture plates and allowed to attach for 24 h. Next, cells were transfected with siRNA and starved for 12 h in a 0.5% serum-containing medium for synchronization. In synchronized cells, EGF was added, incubated for 30 min and treatment with the inhibitors was done for 48 h in 0.5% serum media. Following treatment of 48 h, cells were trypsinized, centrifuged at 650 rcf for 5 min to collect the pellet and again washed with phosphate buffered saline (PBS). Next, for fixation, cells were resuspended in 300 µl PBS and 700 µl chilled ethanol was added dropwise. The fixed cells were stored at -20°C until further analysis. On the day of analysis, cells were washed with chilled PBS and incubated with RNAse for 1 h at 37°C. Cells were then rewashed with PBS, incubated with propidium iodide (PI) and stored in dark on ice until further analysis. BD FacsCalibur flow cytometer was used to analyze the samples and the collected data was further processed and analyzed using FCS Express software.

2.4 Western blotting:

RIPA lysis buffer (Sigma Aldrich) supplemented with protease inhibitor cocktail, sodium fluoride, sodium orthovanadate, phenylmethylsulfonyl fluoride (PMSF) and EDTA was used to extract the total protein from the cells following treatment. The obtained proteins were quantified using bicinchoninic acid (BCA) protein assays reagent, and an equal amount of protein from each sample was loaded for SDS-PAGE. The resolved proteins were subsequently transferred to PVDF membranes. The membranes were treated using blocking buffer (4% BSA in TBST) before being incubated with primary antibodies overnight at 4°C.

Next, the membranes were washed thoroughly using PBST and incubated with a secondary antibody for 3 h at room temperature. The membranes were rewashed thoroughly and further processed for development. The chemiluminescent reagent was used to produce the signals and ChemiDoc (BioRad) was used to record the images. The images were further analyzed using ImageJ software (Fiji). Supplementary **Table. S1** lists the antibodies used along with their source and catalog numbers.

2.5 Generation of spheroids:

3D multicellular tumor spheroids were generated from MDA-MB-231 and MDA-MB-468 cells by the modified forced floating method [13]. Briefly, cells were cultured as monolayers up to confluency, trypsinized, and resuspended in DMEM media. Meanwhile, wells of the 96 well plates were coated with agarose (1% w/v) containing serum-free DMEM media. After that, cells were seeded at a density of 2 x 10^4 cells/well, and centrifuged for 10 min at 700 rcf. Following that, the 96-well plates were incubated for 96 h at 37°C in a humidified environment containing 5% CO_2. With the use of a Nikon Eclipse Ti microscope, the generated spheroids were visually observed and utilized in the following studies.

2.6 Quantitative real-time PCR:

Following treatment of 48 h, RNA was isolated from the cells using Trizol reagent (Sigma). cDNA was generated from the acquired RNA using the iScript cDNA synthesis kit (BioRad) as per the manufacturer guidelines. The cDNA of interest was amplified using a PowerUp™ SYBR™ Green Master Mix (Applied Biosystems) and a Rotor-Gene Q (Qiagen) real-time PCR cycler. The obtained data were normalized to housekeeping gene β-actin and quantified using the delta-delta CT method [14]. Supplementary **Table. S2** lists the sequence of the primers used for amplification. Further, the LinReg PCR software was used to analyze the RT-PCR data.

2.7 Apoptosis assay:

To analyze the early apoptotic, apoptotic and necrotic cell populations, FITC Annexin V Apoptosis Detection Kit (BD Biosciences) was used. After treatment, samples were processed according to the manufacturer's instructions before being examined with a Beckman Coulter CytoFLEX flow cytometer. CytExpert software was used for data analysis and fluorescence compensation correction.

2.8 Live-dead cell imaging and immunofluorescence analysis:

To visualize the live and dead cells after drug treatment, spheroids were washed thrice with PBS and incubated with calcein-AM and PI. The final concentration of calcein-AM and PI used is 2 µM and 4 µM, respectively. Following incubation, spheroids were rewashed thrice with PBS and imaged using Zeiss LSM 880 confocal microscope in addition to Z-stacking analysis.

For immunocytochemistry analysis, cells were treated for 48 h, washed thrice with PBS, fixed with 4% formaldehyde for 15 min and rewashed. To avoid non-specific antibody binding, cells were immersed in blocking buffer for a period of 2 h and further incubated with primary antibodies at 4°C for overnight.

Cells were rewashed, incubated with fluorochrome-conjugated secondary antibodies in the dark at room temperature. After the incubation, cells were washed thrice and counterstained with DAPI. Cells were again washed thrice and finally, imaging was performed using a Zeiss LSM 880 confocal microscope.

2.9 Immunofluorescence flow cytometry:

To perform immunofluorescence flow cytometry, following treatment, cells were washed with PBS, fixed with 4% formaldehyde and rewashed with excess PBS. Next, the cells were resuspended in 1X PBS. Cells were permeabilized by adding 100% chilled methanol slowly to pre-chilled cells, while gently vertexing, to a final concentration of 90% methanol. Following fixation, cells were rewashed in excess PBS, to remove methanol. Next, cells were resuspended in 100 µl of diluted primary antibody, prepared in antibody dilution buffer and incubated overnight at 4°C. Cells were washed thrice in antibody dilution buffer and resuspended in 100 µl of diluted fluorochrome-conjugated secondary antibody. After 2 h of incubation at room temperature, cells were rewashed thrice with antibody dilution buffer and resuspended in 500 µl of antibody dilution buffer. Finally, the cells were analyzed using a CytoFLEX flow cytometer.

2.10 Scratch wound-healing migration assay:

To perform the scratch wound-healing assay, cells were grown to 70–80% confluence in complete DMEM media. Afterward, the media was replaced with 0.5% serum media for a period of 24 h. A linear wound was created by scrapping the cells with a sterile pipette tip to create a wound. To remove the debris, the petri-dish was washed in PBS twice. Images of the wounds were captured before treatment using a Nikon Eclipse Ti microscope. The cells were treated with inhibitors for a period of 18 h. Next, cells were rewashed with PBS to get rid of debris and dead cells. Finally, images of the wounds were captured after treatment. Images of the wounds before and after treatment were analyzed using ImageJ software.

2.11 Matrigel invasion assay:

To assess the change in invasion property following co-treatment, Boyden chamber invasion assay was performed by slight modification of protocol as described by Chen *et al* [15]. Briefly, the upper chamber of the transwell inserts was coated with diluted Matrigel (1 mg/ml in serum-free medium). The coated transwells were incubated at 37°C overnight for solidification. In the upper chamber, 2 x 10^5 cells were seeded in serum-free medium whereas the lower chamber was filled with 750 µl of serum media containing 10% FBS. After incubation of 24 h, the upper side of the chamber was carefully wiped using a wet swab to remove the non-migrated cells and washed thrice with PBS. To fix the migrated cells, the lower part of the chamber was incubated in 4% formaldehyde at 37°C for 15 min. Following fixation, cells were washed thrice with PBS and for visualization stained with DAPI (1 µM). Finally, cells were rewashed thrice in PBS and visualized using Zeiss LSM 880 confocal microscope. The fold change in fluorescence intensity of DAPI represents the alteration of invasion potential. DAPI only stains dsDNA, preventing non-specific staining of the membrane of the transwell.

2.12 Colony formation assay:

The colony formation assay was performed as described by Crowley *et al* [16]. Briefly, cells were seeded in 6-well plates and further treated with siRNA and inhibitors for 48 h, as described earlier. Following treatment, cells were washed with PBS, trypsinized and resuspended in DMEM media. The cells were counted and further resuspended in a fresh medium at 400 cells/mL. 2 mL of cell suspension was added in 6 well culture plates and incubated for a period of 7 days at 37°C. Every alternate 3 days the media was exchanged with fresh media. Further, the formed colonies were washed with PBS, fixed with 100% methanol and stained with 0.5% crystal violet solution. The stained colonies were washed with excess water and dried overnight. Using an inverted brightfield microscope, the colonies were visualized and counted.

2.13 Statistical analysis:

To perform the statistical analysis, GraphPad Prism software was used. All the experimental data are presented as a mean ± standard error of the mean (SEM). The one-way ANOVA and two-way ANOVA tests were performed to look for probable group relationships. A p-value < 0.05 was considered statistically significant where * $p < 0.05$, ** $p < 0.001$, *** $p < 0.001$, **** $p < 0.0001$, respectively.

3 Results

3.1 SQSTM1/P62 and Wnt/β-Catenin are elevated in TNBC tumors and higher expression is associated with poorer prognosis:

To Address the role of SQSTM1/P62 and Wnt/β-Catenin signaling in TNBC, we first examined the messenger RNA expression in a large dataset of TNBC from public databases. We used 'Breast cancer gene-expression miner' (bc-GenExMiner) to analyze the mRNA expression difference between different tumors from the Cancer Genome Atlas (TCGA) database [17]. Bee swarm plot of SQSTM1/P62 and β-Catenin mRNA expression in invasive breast tumors obtained from the Genotype-Tissue Expression (GTEx) and TCGA database displays the significant elevation of expression with respect to healthy tissue **(**Fig. 1a **and b)**. As shown in **(Fig. S1 a)**, the mRNA of SQSTM1/P62 is slightly increased with respect to a non-TNBC tumor. However, β-Catenin is highly expressed in TNBC tumors with respect to non-TNBC tumors **(Fig. S1 b)**. Furthermore, we analyzed the protein expression of SQSTM1/P62 and β-Catenin in breast cancer tissues from the Clinical Proteomic Tumor Analysis Consortium (CPTAC) database using UALCAN portal [18]. Alike the mRNA expression, the protein expression of both SQSTM1/P62 and β-Catenin are elevated in TNBC samples **(**Fig. 1c **and d)**. In addition, we wanted to understand the role of elevated expression of SQSTM1/P62 and β-Catenin on the clinical outcome of the TNBC patients. From the TCGA/GTEx database, 1085 tumor samples and 112 normal samples were analyzed using Gene

Expression Profiling Interactive Analysis 2 (GEPIA 2) portal [19]. From the plots, it can be observed that the higher expression of SQSTM1/P62 and β-Catenin leads to the reduced overall survival of the patients **(Fig. S1 c and d)**. Expression analysis based on cancer stages revealed an increase in SQSTM1/P62 expression with progression to terminal stages **(Fig. S1 e)**. However, β-Catenin is found to decrease with the progression of cancer stages **(Fig. S1 f)**. Altogether, it was observed that the elevated expression of SQSTM1/P62 and Wnt/β-Catenin leads to TNBC progression.

3.2 SQSTM1/P62 and Wnt/β-Catenin are important mediators of stem-like properties of TNBC:

To assess the contribution of SQSTM1/P62 and Wnt/β-Catenin signaling in promoting TNBC stem-like properties, we used siRNA to mediate suppression of SQSTM1/P62 and FH535 to inhibit Wnt/β-Catenin signaling. The efficiencies of SQSTM1/P62 depletion were assessed by western blotting. As shown in Fig. 1 **and Fig. S2**, SQSTM1/P62 was effectively depleted by siRNA in both MDA-MB-231 cells **(**Fig. 1e **and f; Fig. S2 a and b)** and MDA-MB-468 cells **(**Fig. 1h **and l; Fig. S2 d and e)**. Similarly, we analyzed the effect of FH535 on Wnt/β-Catenin signaling. β-Catenin was effectively downregulated by FH535 in both MDA-MB-231 **(**Fig. 1e **and g; Fig. S2 a and c)** and MDA-MB-468 cell lines **(**Fig. 1h **and j; Fig. S2 d and f)**.

To identify cancer stem cells (CSCs) from the main tumor population, cell surface proteins like CD44 and CD24 are utilized. Immuno flow cytometry assay revealed a decrease in the CD44 population and an increase in the CD24 population following co-treatment **(**Fig. 1k **and l)**. Further, we performed colony formation assay and spheroid formation assay, following the inhibition of SQSTM1/P62 and Wnt/β-Catenin signaling in TNBC cells. Knockdown of SQSTM1/P62 and inhibition of the Wnt/β-Catenin pathway reduced the colony formation ability of the TNBC cells. The effect on colony formation was profound in the case of co-treatment in both MDA-MB-468 **(**Fig. 2a **and c)** and MDA-MB-231 **(Fig. S2 g)**. Moreover, the sphere formation ability was dramatically decreased upon SQSTM1/P62 and Wnt/β-Catenin depletion in both MDA-MB-468 **(**Fig. 2b **and d)** and MDA-MB-231 **(Fig. S2 h)**. In addition, qRT PCR was performed to detect the alteration in the gene expression profile of the stemness markers: ALDH1A3 and EpCAM. ALDH1A3 was slightly increased in MDA-MB-231 **(**Fig. 2e**)** and decreased in MDA-MB-468 **(**Fig. 2f**)**, following treatment with FH535 for 48 h. EpCAM was downregulated in MDA-MB-231, while it was found to be upregulated in MDA-MB-468 upon co-treatment **(**Fig. 2e **and f).** Similarly, after treatment for 24 h **(Fig. S3 a and b)**, EpCAM was upregulated in MDA-MB-231 and over-expressed in MDA-MB-468 following co-treatment.

On the other hand, Ki-67 and MDM2 are reported to play important role in maintaining the cancer stem cell niche [20, 21]. Knockdown of SQSTM1/P62 and inhibition of Wnt/β-Catenin effectively decreased the expression of Ki-67 in both TNBC cell lines. The co-treatment resulted in diminished expression of Ki-67, following both 24 h **(Fig. S3 c and d)** and 48 h of treatment **(**Fig. 2g **and h)**. Suppression of SQSTM1/P62 diminished the expression of MDM2 in MDA-MB-231 and MDA-MB-468 **(**Fig. 2g **and h)**. Comparatively, inhibition of Wnt/β-Catenin was less effective in suppressing MDM2 **(**Fig. 2g **and h)**. Similarly, the expression of MDM2 was downregulated following treatment for 24 h **(Fig. S3 c and d)**.

cMYC expression is reported to be positively correlated with self-renewal, chemoresistance and stemness properties of TNBC [22]. Protein expression analysis was carried out to detect the role of SQSTM1/P62 and β-Catenin in maintaining the stemness of TNBC. As shown in Fig. 2i **and k**, depletion of SQSTM1/P62 reduced the cMYC expression in MDA-MB-231 by 2.83-fold. In MDA-MB-468, Wnt/β-Catenin inhibition reduced the cMYC expression by 1.33- fold **(**Fig. 2j **and l)** [23]. Subsequently, after 24 h of treatment, the protein expression level for c-myc was found to be unchanged in MDA-MB-231 **(Fig. S3 i and j)** and was downregulated by 3.33-fold, following co-treatment in MDA-MB-468 **(Fig. S3 k and l).** Moreover, the gene expression profile of c-myc following co-treatment, didn't show any alteration except in MDA-MB-468 treated for 48 h **(Fig. S3 e, f, g and h)**.

The TCF/LEF (T-cell factor/lymphoid enhancer factor) transcription factors are the major end node mediators of the WNT signalling pathway, which exerts its functions upon interacting with the β-catenin [24]. The expression of the following genes was determined by qRT-PCR, which exhibited downregulation of the expression of TCF upon co-treatment in both the cell lines **(Fig. S3 e and f)**. Additionally, the expression of LEF was found to be upregulated following co-treatment in MDA-MB-231, following 24 h and 48 h of treatment **(Fig. S3 e and g)**; whereas it was found to be downregulated following co-treatment for 48 h in MDA-MB-468 **(Fig. S3 f).**

Furthermore, immunocytochemistry revealed downregulation of β-Catenin in MDA-MB-468 **(**Fig. 3**)** and MDA-MB-231 **(Fig. S4)**. Similarly, immunocytochemistry of MDA-MB-231 **(Fig. S5)** and MDA-MB-468 **(Fig. S6)** revealed downregulation of SQSTM1/P62.

3.3 Co-targeting SQSTM1/P62 and Wnt/β-Catenin signaling induce mesenchymal to epithelial transition (MET) in TNBC:

In the process of EMT, tumor-associated epithelial cells obtain mesenchymal features with reduced cell-cell contacts and increased motility, which play critical roles in invasion and metastasis [25]. Given that the suppression of SQSTM1/P62 and Wnt/β-Catenin in monotherapy and combination therapy resulted in diminished stemness of TNBC, we then examined whether knockdown of SQSTM1/P62 and inhibition of Wnt/β-Catenin would affect the metastatic property of TNBC i.e. inhibit the epithelial to mesenchymal transition.

Therefore, qRT-PCR was performed to analyze the alteration in the gene expression profile following co-targeting SQSTM1/P62 and Wnt/β-Catenin signaling. Loss of E-cadherin-mediated adhesion characterizes the transition from benign lesions to invasive, metastatic cancers [26]. On the other hand, Vimentin, N-Cadherin and Fibronectin are highly expressed in mesenchymal cells and are positively correlated with increased metastasis [13]. Following co-targeting signaling pathways, E-cadherin was upregulated by several folds in both TNBC cell lines MDA-MB-231 **(**Fig. 4a**)** and MDA-MB-468 **(**Fig. 4b**)**. Mesenchymal marker Vimentin and N-cadherin and were downregulated by several folds in both the cell lines, following co-therapy **(**Fig. 4a **and b)**. It can be observed that knockdown of SQSTM1/P62 alone was highly effective in diminishing the expression of vimentin **(**Fig. 4a **and b)**. Both knockdown of SQSTM1/P62 and inhibition of Wnt/β-Catenin contributed to the depletion of N-Cadherin in MDA-MB-468

(Fig. 4b). However, blocking the Wnt/β-Catenin signaling was more effective in reducing the expression of Fibronectin over knockdown of SQSTM1/P62 (Fig. 4c **and d)**.

Caveolin-1 plays a positive regulatory effect on TNBC invasion and metastasis [27]. Similar to other EMT factors, it was also downregulated following co-modulation of the pathways (Fig. 4c **and d)**. Nonetheless, co-treatment reduced the expression of mesenchymal markers effectively.

EMT is orchestrated by a restricted number of transcription factors mainly the three: SNAIL, Twist, and Zeb families, which are able to promote the repression of epithelial features and induction of mesenchymal features [28]. Hence, suppression of SQSTM1/P62 and Wnt/β-Catenin reduced the expression of Twist1 and SNAIL by 2.2-fold and 3.05-fold (Fig. 4e **and f).** It can be noticed that SQSTM1/P62 knockdown was more effective in downregulating Twist1 than the co-treatment (Fig. 4e**).**

Furthermore, protein expression analysis was performed by Western blot. As shown in (Fig. 4g, h **and i, j)**, E-cadherin expression was significantly induced by knockdown of SQSTM1/P62 in both TNBC cell lines MDA-MB-231 and MDA-MB-468. However, treatment with FH535 resulted in a decrease in E-cadherin expression. It also contributed to reduced E-cadherin expression in the case of co-treatment.

Moreover, mesenchymal marker vimentin was effectively depleted following knockdown of SQSTM1/P62 in both the cell lines (Fig. 4k **and l)**. A similar effect was also observed in the case of β-Catenin down-regulation (Fig. 4k **and l)**. Similar to individual treatment, co-treatment effectively downregulated vimentin expression.

Similarly, following treatment for 24 h the expression analysis of the aforementioned genes were also analysed. It was observed that there was a concomitant reduction in the expression of the EMT markers and transcription factors in both the TNBC cell lines **Fig. S7**. On one hand E-cadherin was found to be upregulated in both the cell lines following co-treatment **(Fig. S7 a and b)**, while Vimentin, fibronectin, N-cadherin was found to be downregulated following treatments with the inhibitors alone and in combination **(Fig. S7 a, b, c and d)**. Additionally, the expression of the EMT transcription factors (SNAIL, and Twist1) was also found to be downregulated significantly **(Fig. S7 e and f)**. The E-cadherin protein expression was also found to be upregulated tremendously in siRNA treated cells. However, the co-treatment failed to induce the expression of E-cadherin protein significantly in MDA-MB-231**(Fig. S7 g and h)**, whereas there was a reduction in the E-cadherin protein expression following co-treatment in MDA-MB-468 cell line **(Fig. S7 i and j)**. Further, the histogram plots depicted a reduction in the expression of the mesenchymal marker, Vimentin in MDA-MB-468 cells, while not much difference in the levels was observed in case of MDA-MB-231 cells **(Fig. S7 k and l).**

Next, we analyzed the alteration of the expression level of transcription factors contributing to EMT. The expression of Twist1 was diminished following co-treatment in both TNBC cell lines MDA-MB-231 and MDA-MB-468, after 48 h of treatment (Fig. 5a, b **and e, f)**. The same was observed in MDA-MB-468 24 h treatment **(Fig. S8 d and e)**. However, the expression of Twist1 was found to be upregulated by 2.1-fold, following co-treatment for 24h in MDA-MB-231 **(Fig. S8 a and b).** Although, Knockdown of SQSTM1/P62

contributed to a reduction of Twist1, the effect of inhibition of Wnt/β-Catenin signaling was more profound. Additionally, in MDA-MB-231, SQSTM1/P62 knockdown resulted in a reduction in ZEB expression **(**Fig. 5a **and c)**. Alteration of SQSTM1/P62 and Wnt/β-Catenin signaling had no effect on the expression of SNAIL in MDA-MB-231 **(**Fig. 5a **and d)**. However, in MDA-MB-468 the SNAIL was effectively reduced by co-targeting, following 24 h **(Fig. S8 d and f)** and 48 h of treatment **(**Fig. 5e **and g)**.

Besides analyzing the changes of protein expression in monolayer culture, the effect of the combination was also examined in tumor spheroids which mimics the solid tumors. Unlike the monolayer culture, knockdown of SQSTM1/p62 reduced the expression of SNAIL in MDA-MB-231 3D spheroids **(**Fig. 5h **and i)**. Although Wnt/β-Catenin signaling inhibition increased the E-cadherin in MDA-MB-468, the co-treatment couldn't increase the expression **(**Fig. 5j **and k)**. Also, the expression of Twist1 was found to be slightly increased **(**Fig. 5j **and l)**.

To visualize the alteration of expression of E-cadherin and vimentin, immunocytochemistry was performed on both the TNBC cell lines. E-cadherin was found to be upregulated following co-treatment in both MDA-MB-231 **(Fig. S9)** and MDA-MB-468 **(Fig. S10)**. On the other hand, vimentin was also found to be downregulated in both the cell lines **(**Fig. 6 **and Fig. S11).**

Altogether, these findings indicate that co-targeting SQSTM1/P62 and Wnt/β-Catenin signaling induces MET, with a concomitant reductions in the metastatic potentials of TNBC cells.

3.4 Suppression of SQSTM1/P62 and Wnt/β-Catenin signaling decreases the migration and invasion potential of TNBC:

During the process of EMT, epithelial cells reverse their morphology into mesenchymal cells and gain increased abilities for migration and invasion, which could result in metastasis [25]. Since increased expression of SQSTM1/P62 and Wnt/β-Catenin are implicated in the migration and invasion of TNBC cells, we next investigated the combined effect of suppression of SQSTM1/P62 and Wnt/β-Catenin signaling on the migration and invasion of MDA-MB-231 cells. Migration was assessed using a scratch wound-healing assay, where the migration rate of the cells towards the wound area (created using a scratch) was determined. We found that the cells incubated with FH535, siRNA for SQSTM1/P62 and in combination showed slower wound healing abilities than the untreated cells **(**Fig. 7b **and e; Fig. S12 b and d)**. The rate of cell migration was found to be lower in SQSTM1/P62 knockdown cells compared to Wnt/β-Catenin inhibited cells and lowest in the combination treatment. In addition, a Boyden chamber-based assay, in which cells invade a layer of Matrigel on top of a membrane, was used to monitor the invasive capacity of MDA-MB-231 and MDA-MB-468 cells. After 24 h, a 5.22 and 3.68-fold reduction in invasion capacity was observed in cells treated with the combination of FH535 and siRNA compared to the untreated cells **(**Fig. 7a **and d; Fig. S12 a and c)**. Of note, the effect on migration and invasion was stronger upon co-treatment compared to treatment with individual agent, confirming the synergistic effect of the suppression of SQSTM1/P62 and Wnt/β-Catenin signaling **(**Fig. 7a **and b; Fig. S12 a and b)**.

Conclusively, these data indicate that co-inhibition of SQSTM1/P62 and Wnt/β-Catenin signaling reduces the migration and invasion capacities of TNBC cells.

3.5 Inactivation of SQSTM1/P62 and Wnt/β-Catenin signaling alters the expression of ABC transporters:

Drug efflux transport systems have extensively been studied owing to the phenomenon of MDR, in which cancer cells become cross-resistant to multiple cytotoxic anticancer drugs [29]. MDR often results from the overexpression of ABC transporters [30]. This prompted us to study alterations in the expression of the MDR genes: ABC subfamily B member 1 (ABCB1; also called P-glycoprotein), ABC subfamily C member 1 (ABCC1; also called MDR-associated protein 1), ABC subfamily G member 2 (ABCG2; also called breast cancer resistance protein), by qRT-PCR. In Fig. 7f **and g**, the expression levels of the ABC transporters in MDA-MB-231 and MDA-MB-468 are depicted, following 48 h of treatment. We found that combination treatment led to a decreased ABCB1 expression in both MDA-MB-231 and MDA-MB-468. However, FH535 treatment alone increased ABCB1 expression by 2.22-fold and 1.33-fold in MDA-MB-231 and MDA-MB-468, respectively. After combination treatment, the expression of ABCG2 was found to be reduced significantly in MDA-MB-468 but was slightly increased in MDA-MB-231. In fact, FH535 treatment increased ABCG2 expression in MDA-MB-231 by 3.67-fold. Although co-treatment decreased the ABCC1 expression in MDA-MB-231, it was unaltered in MDA-MB-468. Similarly, after 24 h of treatment, the expression of ABCG2 was found to be downregulated in both the cell lines. However, the expression of ABCB1 and ABCC1 was found to be upregulated following co-treatment, except in siRNA treated cells, which was found to be downregulated in both the cell lines **(Fig. S12 e and f)**. Altogether, these data indicate that the inactivation of SQSTM1/P62 and Wnt/β-Catenin signaling alters the expression of major MDR-associated genes in TNBC cells.

3.6 Co-targeting SQSTM1/P62 and Wnt/β-Catenin signaling synergistically inhibit TNBC cell survival:

To discern the effect of inhibition of SQSTM1/P62 and Wnt/β-Catenin signaling on cell survival, alamarBlue based cell viability assay was performed. We observed a dose-dependent decrease in cell viability following treatment with Wnt/β-Catenin inhibitor FH535 in both the TNBC cell lines MDA-MB-231 and MDA-MB-468 **(Fig. S13)**. A several-fold higher dose of FH535 was required for the spheroids **(Fig. S14)**. On the other hand, we didn't observe any effect on cell viability following the knockdown of SQSTM1/P62. Even transfection of a higher concentration of siRNA had no effect on cell viability both in monolayer cultures and spheroids. Surprisingly, the combination of FH535 with siRNA was found to decrease cell viability significantly in a dose-dependent manner at lower concentrations in both monolayers and spheroids. The combination index (CI) calculation revealed a CI value of < 1 for both cases, indicating a dose-dependent synergistic interaction between SQSTM1/P62 and Wnt/β-Catenin signaling inhibition. Administration of the inhibitor and siRNA in combination yielded higher anti-proliferative effects than when administered alone **(Fig. S13)**. In the case of spheroids, a relatable finding was observed as well **(Fig. S14)**.

Furthermore, live-dead cell imaging of spheroids following treatment provided a clear visualization of the effect of the signaling modulation (Fig. 7c and S15). Fluorescence intensities of the spheroids presented in, which depicts a markedly induced disintegration of the spheroids **(Fig. S15)**. Taken together, these data indicate that attenuation of SQSTM1/P62 and Wnt/β-Catenin signaling synergistically inhibits TNBC cell survival.

3.7 Modulation of SQSTM1/P62 and Wnt/β-Catenin signaling results in G0/G1 phase cell cycle arrest and induces apoptosis:

To better document the effect of inhibition of SQSTM1/P62 and Wnt/β-Catenin signaling on cell growth/survival, cell cycle progression was monitored following 48 h treatment. A G0/G1 phase cell cycle arrest was observed in both MDA-MB-231 and MDA-MB-468. The percentage of G0/G1 phase cells was increased to 27.27% in MDA-MB-231 (Fig. 7h) and 22.6% in MDA-MB-468 (Fig. 7i). Cyclin-D1 is a regulatory protein responsible for driving cell cycle progression from the G1 to S phase [31]. Thus, we set out to analyze the expression levels of cyclin-D1 using qRT-PCR to better understand the mechanism of action of the inhibitors. The expression levels of cyclin-D1 were found to be down-regulated by 2.67-fold in MDA-MB-231 cells (Fig. 7j **and k)**.

Following the reduction of cell viability by co-treatment, we wanted to know if the cell death was mechanized by the apoptotic process. Thus, we analyzed the increase in the percentage of apoptotic cell population following combination treatment using flow cytometry. It was observed that co-therapy increased apoptotic cell populations by approximately 26.81% and 23.13% in MDA-MB-231 (Fig. 8a) and MDA-MB-468 **(Fig. S16a)**, respectively.

Therefore, we conclude that modulation of the SQSTM1/P62 and Wnt/β-Catenin signaling pathway ablates cyclin-D1, leading to G0/G1 cell cycle arrest. Furthermore, it also mediates apoptotic cell death.

3.8 Knockdown of SQSTM1/P62 results in inactivation of non-canonical Wnt VANGL2-JNK signaling axis:

Besides canonical Wnt/β-Catenin signaling, the non-canonical Wnt signaling is also implicated in TNBC aggressiveness [32]. TNBC cells orchestrate their evasive property via the planar cell polarity pathway or Wnt VANGL2-JNK signaling axis [33]. Therefore, further studies were carried out to examine the impact of combination treatment on this signaling pathway. It was observed that the inhibition of SQSTM1/P62 or Wnt/β-Catenin signaling didn't alter the expression of VANGL2 in both the TNBC cells lines following treatment for a period of 24 h **(Fig. S16 b and c)** and 48 h **(Fig. S16 d and e)**. However, the knockdown of SQSTM1/P62 decreased p-JNK in both MDA-MB-231 (Fig. 8b **and d)** and MDA-MB-468 (Fig. 8c **and e)**, following 48 h of treatment. Moreoever, similar effects was observed after 24 h of treatment in both MDA-MB-231 **(Fig. S16 f and h)** and MDA-MB-468 **(Fig. S16 g and i)**.

In immunocytochemistry, VANGL2 and SQSTM1/P62 are detected to be colocalized in punctate cytoplasmic patterns in late endosomal compartments of both TNBC cell lines **(Fig. S17 and S18).** As expected, the colocalization is not visible in SQSTM1/P62 knockout cells.

3.9 Suppression of SQSTM1/P62 does not alter NF-κβ expression but depletes activated form of AKT:

Next, we wanted to examine if SQSTM1/P62 had any role in the stability of NF-κβ. Thus, the protein expression of total NF-κβ was evaluated following knockdown of SQSTM1/P62 and inhibition of Wnt/β-Catenin signaling. Immuno-flowcytometry revealed unaltered NF-κβ expression following both 24 h **(Fig. S19 a and b)** and 48 h **(Fig. S19 c and d)** of treatment. Furthermore, we wanted to know the effect of co-treatment on the PI3K/AKT/mTOR signaling pathway. Western blot revealed depletion of the activated form of AKT i.e. phospho AKT following knockdown of SQSTM1/P62 by siRNA in both MDA-MB-231 **(**Fig. 8f **and h; Fig. S19 e and g)** and MDA-MB-468 **(**Fig. 8g **and i; Fig. S19 f and h)**. However, inhibition of Wnt/β-Catenin signaling by FH535 didn't alter the expression of pAKT. Confocal images of immunofluorescence cytometry confirmed the SQSTM1/P62-siRNA mediated repression of pAKT in both MDA-MB-231 **(Fig. S20)** and MDA-MB-468 **(Fig. S21)**.

3.10 Alteration of Wnt/β-Catenin signaling down-regulates activated form of STAT-3 but co-treatment does not alter MAPK expression:

Clinical and preclinical data indicate the involvement of overexpressed and constitutively activated STAT-3 and ERK-1/2 in the progression, proliferation, metastasis and chemoresistance of TNBC [34, 35]. Protein expression analysis revealed knockdown of SQSTM1/P62 has almost no effect on the expression of pSTAT-3 or pERK-1/2 in both cell lines **(**Fig. 8j **and k)**. However, inhibition of Wnt/β-Catenin signaling by FH535 effectively reduced the expression of pSTAT-3 by 3.22-fold and 3.9-fold in MDA-MB-231 and MDA-MB-468, respectively **(**Fig. 8l **and m)**. Treatment with FH535 slightly increased the pERK-1/2 **(**Fig. 8j **and k)**. In fact, co-treatment increased the expression of pERK-1/2 marginally **(**Fig. 8n **and o)**.

Subsequently, following 24 h of treatment, no such changes in the expression of pSTAT-3 was observed following co-treatment **(Fig. S22 a, b, d and e).** However, there was a significant reduction in the expression profile of the gene following treatment with FH535 in both the cell lines **(Fig. S22 b and e).** Similarly, co-treatment induced the expression of p-MAPK by 1.67-fold in MD-MB-468 cells **(Fig. S22 d, f)**, while it remained unchanged in MDA-MB-231 cells **(Fig. S22 a, c).**

Immunocytochemistry revealed downregulation in the expression of phospo-STAT3, following treatment in both MDA-MB-231 **(Fig. S23)** and MDA-MB-468 **(Fig. S24)** cells.

3.11 EMT induction by EGF induces autophagy and inhibition of Wnt/β-Catenin signaling by FH535 repress autophagic activity:

Next, we wanted to document the effect of suppression of SQSTM1/P62 and Wnt/β-Catenin signaling in the autophagic activity of TNBC cells. Following EMT induction the LC3 II/1 ratio increased indicating induction of autophagic activity. We didn't observe a significant change in the LC3 II/1 ratio when cells were treated for a period of 48 h **(**Fig. 8p, r, q **and s)**. However, significant inhibition of autophagic activity by FH535 was observed in MDA-MB-468 when cells were treated for a period of 24 h **(Fig. S25 e)**.

4 Discussion

Several signaling pathways have been implicated in maintaining EMT and stemness of TNBC cells. An array of crosstalks, feedback mechanisms, as well as their critical involvement in the normal cellular developmental process, renders it challenging to successfully target them and prevent EMT. Therefore, to combat EMT and stemness of TNBC, the crosstalk between signaling pathways has to be obliterated. By mining a large dataset on TNBC from public databases, we have shown that the mRNA and protein expression of both β-catenin and SQSTM1/P62 are elevated in TNBC tumors in comparison to the non-TNBC tumors. From the Kaplan-Meier survival analysis, it can be observed that higher expression of SQSTM1/P62 and β-Catenin leads to the reduced overall survival of the TNBC patients. Similarly, SQSTM1/P62 expression is found to be elevated with the progression of cancer stages.

Given the strong correlation of Wnt/β-catenin signaling and SQSTM1/P62 in TNBC pathogenesis, we tried to elucidate the critical roles played by these two pathways in TNBC progression. Earlier reports suggest that Wnt/β-catenin signaling contributes to the stemness of TNBC. TCF and LEF mediate Wnt signals, and the overactive Wnt signal drives TCF/LEF to transform cells and induce stem cell-like properties [8]. Similarly, reports by Xu et al. suggest that SQSTM1/P62 enhances breast cancer stem-like properties [36]. Suppression of Wnt/β-catenin and SQSTM1/P62 reduced the expression of TCF and LEF. Furthermore, the inhibition of Wnt/β-catenin signaling and silencing of SQSTM1/P62 led to reduced sphere-forming and colony-forming ability suggesting Wnt/β-catenin and SQSTM1/P62 as a potential target to limit TNBC stemness. Additionally, we looked into the gene expression alteration of CSC markers to validate our findings. Soysal et al. reported that EpCAM is highly expressed in TNBC and positively correlated with TNBC lymph node metastasis and distant metastasis [37]. Moreover, higher EpCAM expression corresponds to CSC population generation through OCT4, NANOG, c-MYC, and SOX2 [38]. ALDH1A3 a CSC biomarker is abundantly expressed in cancer stem cells, which have significant resistance towards treatment, besides possessing the ability to induce clonogenic development, and tumor-initiating potential [39]. It was observed that after treatment, ALDH1A3 was reduced by 1.76-fold in MDA-MB-468. EpCAM was reduced by 5.35-fold by knockdown of SQSTM1/P62 in MDA-MB-231 and

remained almost unaltered in MDA-MB-468. In addition to stemness markers, we analyzed the expression of genes responsible for promoting and maintaining cancer stem cells. Reports by Cidado et al. suggest that Ki-67 is required to maintain cancer stem cells but not cell proliferation [20]. Wienken et al. described the role of MDM2 in maintaining stemness and cancer cell survival via stabilizing histone modifications, such as H2AK119ub1 and H3K27me3 [40]. The results in our study depicts that co-treatment reduced the expression of both Ki-67 and MDM2, and the knockdown of SQSTM1/P62 depleted MDM2 expression. Karin et al. reported that SQSTM1/P62-mediated activation of Nrf2 triggers MDM2 expression in premalignant pancreatic intraepithelial neoplasia 1, supporting our finding [41]. The transcription factor cMYC is known to cooperate with HIF2α, a stemness-associated transcription factor that increases self-renewal of embryonic stem cells through coordinated upregulation of Oct-4 and Nanog [42]. Protein expression analysis revealed that knockdown of SQSTM1/P62 decreased the expression of cMYC by 2.9-fold in MDA-MB-231. Similar to our finding, Xu et al. has reported that SQSTM1/P62 enhances breast cancer stem-like properties by stabilizing MYC mRNA at the post-transcriptional level, rather than influencing its promoter activity [36].

EMT is induced in tumor cells during metastasis and invasion, allowing cells to detach from the basement membrane and link with other cells, allowing them to spread beyond their initial location and infiltrate nearby organs [25]. Since Wnt/β-catenin and SQSTM1/P62 are known to contribute to EMT progression, the effect of their modulation was evaluated. Following treatment with FH535 and siRNA, the upregulation of epithelial marker E-cadherin and downregulation of mesenchymal marker Vimentin, N-cadherin, Fibronectin and Caveolin-1 indicates the phase transition from EMT to MET. The experimental data shows that knockdown of SQSTM1/P62 upregulated the expression of E-cadherin in both TNBC cell lines. Damiano et al. has reported that SQSTM1/P62 interacts with E-cadherin and delivers it to autophagosome for degradation which supports the experimental finding [43]. Furthermore, reports by Li et al. states that SQSTM1/P62 interacts with Vimentin and positively upregulates its expression [44]. Similarly, Gilles et al. has shown that β-catenin/TCF could directly transactivate Vimentin [45]. Herein, the decreased level of Vimentin after FH535 and siRNA treatment correlates with these studies. Moreover, the transcription factor Twist1 was downregulated by knockdown of SQSTM1/P62 in both MDA-MB-231 and MDA-MB-468. In line with our finding, Quing et al. found that autophagy deficiency promotes cell proliferation and migration through SQSTM1/P62-dependent stabilization of the oncogenic transcription factor Twist1. SQSTM1/P62 binds to Twist1 and inhibits degradation of Twist1 [46]. Activation of the Wnt/β-catenin signaling pathway is known to contribute to cervical cancer pathogenesis via upregulation of Twist1 [47]. Similar to these findings, treatment with FH535 was found to effectively downregulate Twist1 expression. Silencing SQSTM1/P62 didn't alter the SNAIL expression in MDA-MB-231 and MDA-MB-468 monolayer. Strikingly, SNAIL was almost depleted in SQSTM1/P62 knockdown spheroids. Bertrand et al. has shown that inhibition of SQSTM1/P62 expression by siRNA strongly decreased SNAIL level after EMT induction [7]. Therefore, the experimental findings indicate the pivotal role played by Wnt/β-catenin and SQSTM1/P62 pathway in regulating EMT in TNBC.

Overexpression of SQSTM1/P62 is known to promote cell migration in hepatocellular carcinoma via activation of the Wnt/β-Catenin pathway [48]. Similarly, in TNBC cells line MDA-MB-231 and MDA-MB-

468, modulation of Wnt/β-Catenin pathway and SQSTM1/P62 reduced the migration and invasion potential.

Multidrug resistance (MDR), which is primarily caused by overexpression of ATP-binding cassette (ABC) transporters, is a significant impediment to effective chemotherapy treatment [49]. Indeed, the Wnt/β-catenin pathway has been reported to regulate ABCB1 transcription in chronic myeloid leukemia [50]. Alteration of the Wnt/β-Catenin pathway and SQSTM1/P62 effectively reduced the expression of ABC transporters signifying the positive correlation between the pathways and ABC transporters.

Cyclin-D1 promotes cell cycle progression from G1 to S phase by phosphorylating and inactivating the retinoblastoma (Rb) protein, which releases E2F transcription factors [51]. Tetsu et al. found that β-catenin controls Cyclin-D1 expression in colon cancer cells and that aberrant β-catenin expression levels can lead to Cyclin-D1 accumulation, which can lead to neoplastic transformation [52]. Qi et al. reported that SQSTM1/P62 regulates breast cancer progression and metastasis by inducing cell cycle arrest and regulating immune cell infiltration [53]. Evidently, modulation of the Wnt/β-catenin signaling pathway and SQSTM1/P62 resulted in reduced expression of Cyclin-D1, leading to G0/G1 cell cycle arrest. The propensity of an anticancer medicine to induce apoptosis in the targeted cells determines its cytotoxicity. The increase in 26.81% and 23.13% apoptotic cell populations in MDA-MB-231 and MDA-MB-468 implies the importance of these pathways in TNBC survival.

The Wnt/PCP protein VANGL2 is found to be overexpressed in TNBC. Furthermore, SQSTM1/P62 is required to recruit and activate JNK in breast cancer cells through VANGL2- SQSTM1/P62 signaling cascade. SQSTM1/P62 recruits JNK to VANGL2 and contributes to its activation [54]. Therefore, knockdown of SQSTM1/P62 results in inactivation of non-canonical Wnt VANGL2-JNK signaling axis and reduces activated form of JNK in both cell lines.

Schwob et al. reported unaltered expression of NF-κβ following SQSTM1/P62 silencing [55]. Herein, no change in NF-κβ expression was detected by alteration of SQSTM1/P62. However, western blot revealed depletion of the activated form of AKT i.e. phospho AKT, following knockdown of SQSTM1/P62 by siRNA. A plausible explanation for this phenomenon may be linked to PKCzeta, which is known to be a negative regulator of AKT activation. Joung et al. found that SQSTM1/P62 dependent AKT phosphorylation occurred via the release of AKT from PKCzeta by the association of SQSTM1/P62 and PKCzeta [56].

Through GSK3β, the Wnt/β-catenin pathway forms a bidirectional positive feedback loop involving MAPK and STAT3 [57]. MAPK and STAT-3 have been implicated in EMT in prior studies [58]. After incubation with the inhibitor/siRNA, the expression of pMAPK and pSTAT-3, both important downstream components of cell survival signaling pathways, decreased, indicating the intricacy and web-like interconnectedness between the receptors studied and the suppression of EMT and growth signals.

Induction of EMT by EGF was found to induce autophagy. Similarly, inhibition of Wnt/β-Catenin signaling by FH535 repressed autophagic activity. Earlier studies by Kuhn et al. also indicated Wnt/β-Catenin

mediated decrease in autophagic activity [59]. Knockdown of SQSTM1/P62 by siRNA did not affect the autophagic activity of TNBC cells. Korolchuk et al. found that LC-3 conversion was not significantly changed by either knockdown or overexpression of SQSTM1/P62, indicating that SQSTM1/P62 does not alter autophagic activity under normal conditions [60]. Hence, these findings are clear indicators of the pivotal role played by the Wnt/β-Catenin signaling pathway and SQSTM1/P62 in TNBC survival through downstream signaling.

5 Conclusion

The key drivers of therapeutic resistance in TNBC include anomalous EMT activation and associated cancer stem cell-like characteristics. In search of successful therapy, autophagy adaptor protein SQSTM1/P62 and Wnt/β-Catenin pathway, two important signaling pathways governing EMT were targeted. In conjunction with reversal of EMT phenotype by co-treatment, genes involved in cancer stemness and MDR was similarly reduced. Furthermore, impeding EMT inhibited TNBC cell migration and invasion. Nonetheless, by targeting numerous signaling nodes and limiting downstream crosstalk, the suggested combination treatment was able to avoid most of the issues concerning EMT regulation.

Declarations

6.1 Ethical Approval and Consent to participate:

Not applicable.

6.2 Consent for publication:

Not applicable.

6.3 Availability of supporting data:

All the supporting data are available in electronic file format as supplementary material file.

6.4 Competing interests:

The authors declare that they do not have any conflicts of interest.

6.5 Funding:

The study was supported by the Department of Biotechnology (BT/PR44695/NER/95/1880/2021 and BT/PR41449/NER/95/1687/2020) at DBT Programme Support Facility, IIT Guwahati. Partial support of ICMR Centre for Excellence, Grant no. 5/3/8/20/2019-ITR, INUP, MeitY Grant no. 5(1)/2021-NANO) are also acknowledged.

6.6 Authors' contributions:

RS Contributed to conceptualization, methodoly development and optimization, formal analysis and investigation, manuscript preparation, review and editing. PS helped in manuscript editing and experiments. SSG contributed to conceptualization, supervision and resource allocation.

6.7 Acknowledgements:

The authors acknowledge the DBT program Support Facility, Centre for Nanotechnology, Department of Electronics and Information Technology grant, and the Central Instruments Facility (CIF), School of Heath Sciences,IIT Guwahati, India.

Authors' information:

Department of Biosciences and Bioengineering, Indian Institute of Technology Guwahati, Guwahati-39, Assam, India.

Rajib Shome, Plaboni Sen, Siddhartha Sankar Shosh

Centre for Nanotechnology, Indian Institute of Technology Guwahati, Guwahati-39, Assam, India

Siddhartha Sankar Shosh

Corresponding Author:

Correspondence to Siddhartha Sankar Shosh

Email: sghosh@iitg.ac.in

Phone: +0361-258-2206

Fax: +0361-258-2249

ORCID ID: 0000-0002-7121-5610

References

1. J.M. Lee, S. Dedhar, R. Kalluri, E.W. Thompson, The epithelial–mesenchymal transition: new insights in signaling, development, and disease. J. Cell Biol. **172**, 973–981 (2006)
2. N. Shekar, P. Mallya, D. Gowda, V. Jain, Triple-negative breast cancer: challenges and treatment options. (2020)
3. C. Anders, L.A. Carey, Understanding and treating triple-negative breast cancer. Oncol. (Williston Park NY) **22**, 1233 (2008)
4. E.M. De Francesco, F. Sotgia, M.P. Lisanti, Cancer stem cells (CSCs): metabolic strategies for their identification and eradication. Biochem. J. **475**, 1611–1634 (2018)

5. P. Sánchez-Martín, M. Komatsu, p62/SQSTM1–steering the cell through health and disease. J. Cell. Sci. **131**, jcs222836 (2018)
6. M. Gugnoni, V. Sancisi, G. Manzotti, G. Gandolfi, A. Ciarrocchi, Autophagy and epithelial–mesenchymal transition: an intricate interplay in cancer. Cell. Death Dis. **7**, e2520–e2520 (2016)
7. M. Bertrand, V. Petit, A. Jain, R. Amsellem, T. Johansen, L. Larue, P. Codogno, I. Beau, SQSTM1/p62 regulates the expression of junctional proteins through epithelial-mesenchymal transition factors. Cell. Cycle **14**, 364–374 (2015)
8. R. Fodde, T. Brabletz, Wnt/β-catenin signaling in cancer stemness and malignant behavior. Curr. Opin. Cell. Biol. **19**, 150–158 (2007)
9. A.M. Daulat, J.-P. Borg, Wnt/planar cell polarity signaling: new opportunities for cancer treatment. Trends in cancer **3**, 113–125 (2017)
10. K. VanderVorst, C. Dreyer, J. Hatakeyama, G.R. Bell, A.L. Berg, M. Hernandez, H. Lee, S.R. Collins, K.L. Carraway, Wnt/PCP signaling mediates breast cancer metastasis by promoting pro-invasive protrusion formation in collectively motile leader cells. bioRxiv (2022)
11. J. O'brien, I. Wilson, T. Orton, F. Pognan, Investigation of the Alamar Blue (resazurin) fluorescent dye for the assessment of mammalian cell cytotoxicity. Eur. J. Biochem. **267**, 5421–5426 (2000)
12. T.-C. Chou, Drug combination studies and their synergy quantification using the Chou-Talalay method. Cancer Res. **70**, 440–446 (2010)
13. R. Shome, S.S. Ghosh, Tweaking EMT and MDR dynamics to constrain triple-negative breast cancer invasiveness by EGFR and Wnt/β-catenin signaling regulation. Cell. Oncol. **44**, 405–422 (2021)
14. X. Rao, X. Huang, Z. Zhou, X. Lin, An improvement of the 2ˆ (−delta delta CT) method for quantitative real-time polymerase chain reaction data analysis. Biostatistics Bioinf. biomathematics **3**, 71 (2013)
15. H.-C. Chen, *Cell migration* (Springer, 2005), pp. 15–22
16. L.C. Crowley, M.E. Christensen, N.J. Waterhouse, Measuring survival of adherent cells with the colony-forming assay. Cold Spring Harbor Protocols 2016, pdb. prot087171 (2016)
17. P. Jézéquel, J.-S. Frénel, L. Campion, C. Guérin-Charbonnel, W. Gouraud, G. Ricolleau, M. Campone, bc-GenExMiner 3.0: new mining module computes breast cancer gene expression correlation analyses. Database 2013, (2013)
18. U. Chandrashekar, A Portal for Facilitating Tumor Subgroup Gene Expression and Survival Analyses. Neoplasia
19. Z. Tang, B. Kang, C. Li, T. Chen, Z. Zhang, GEPIA2: an enhanced web server for large-scale expression profiling and interactive analysis. Nucleic Acids Res. **47**, W556–W560 (2019)
20. J. Cidado, H.Y. Wong, D.M. Rosen, A. Cimino-Mathews, J.P. Garay, A.G. Fessler, Z.A. Rasheed, J. Hicks, R.L. Cochran, S. Croessmann, Ki-67 is required for maintenance of cancer stem cells but not cell proliferation. Oncotarget **7**, 6281 (2016)
21. H.A. Abbas, D.R. Maccio, S. Coskun, J.G. Jackson, A.L. Hazen, T.M. Sills, M.J. You, K.K. Hirschi, G. Lozano, Mdm2 is required for survival of hematopoietic stem cells/progenitors via dampening of

ROS-induced p53 activity. Cell. stem cell. **7**, 606–617 (2010)

22. S. Yin, V.T. Cheryan, L. Xu, A.K. Rishi, K.B. Reddy, Myc mediates cancer stem-like cells and EMT changes in triple negative breast cancers cells. PLoS One **12**, e0183578 (2017)
23. W. Li, H. Ma, J. Zhang, L. Zhu, C. Wang, Y. Yang, Unraveling the roles of CD44/CD24 and ALDH1 as cancer stem cell markers in tumorigenesis and metastasis. Sci. Rep. **7**, 1–15 (2017)
24. K.M. Cadigan, M.L. Waterman, TCF/LEFs and Wnt signaling in the nucleus. Cold Spring Harb. Perspect. Biol. **4**, a007906 (2012)
25. J. Yang, P. Antin, G. Berx, C. Blanpain, T. Brabletz, M. Bronner, K. Campbell, A. Cano, J. Casanova, G. Christofori, Guidelines and definitions for research on epithelial–mesenchymal transition. Nat. Rev. Mol. Cell Biol. **21**, 341–352 (2020)
26. N. Pećina-Šlaus, Tumor suppressor gene E-cadherin and its role in normal and malignant cells. Cancer Cell. Int. **3**, 1–7 (2003)
27. X.-L. Qian, Y.-H. Pan, Q.-Y. Huang, Y.-B. Shi, Q.-Y. Huang, Z.-Z. Hu, L.-X. Xiong, Caveolin-1: a multifaceted driver of breast cancer progression and its application in clinical treatment. Onco Targets Ther. **12**, 1539 (2019)
28. S. Ansieau, G. Collin, L. Hill, EMT or EMT-promoting transcription factors, where to focus the light? Front. Oncol. **4**, 353 (2014)
29. B. Mansoori, A. Mohammadi, S. Davudian, S. Shirjang, B. Baradaran, The different mechanisms of cancer drug resistance: a brief review. Adv. Pharm. Bull. **7**, 339 (2017)
30. D. Theile, P. Wizgall, Acquired ABC-transporter overexpression in cancer cells: transcriptional induction or Darwinian selection? Naunyn-schmiedeberg's. Archives of Pharmacology **394**, 1621–1632 (2021)
31. L. Ding, J. Cao, W. Lin, H. Chen, X. Xiong, H. Ao, M. Yu, J. Lin, Q. Cui, The roles of cyclin-dependent kinases in cell-cycle progression and therapeutic strategies in human breast cancer. Int. J. Mol. Sci. **21**, 1960 (2020)
32. X. Xu, M. Zhang, F. Xu, S. Jiang, Wnt signaling in breast cancer: biological mechanisms, challenges and opportunities. Mol. Cancer **19**, 1–35 (2020)
33. E. Martin-Orozco, A. Sanchez-Fernandez, I. Ortiz-Parra, A.-S. Nicolas, WNT signaling in tumors: the way to evade drugs and immunity. Front. Immunol. 2854 (2019)
34. J.M. McDaniel, K.E. Varley, J. Gertz, D.S. Savic, B.S. Roberts, S.K. Bailey, L.A. Shevde, R.C. Ramaker, B.N. Lasseigne, M.K. Kirby, Genomic regulation of invasion by STAT3 in triple negative breast cancer. Oncotarget **8**, 8226 (2017)
35. G. Palma, G. Frasci, A. Chirico, E. Esposito, C. Siani, C. Saturnino, C. Arra, G. Ciliberto, A. Giordano, M. D'Aiuto, Triple negative breast cancer: looking for the missing link between biology and treatments. Oncotarget **6**, 26560 (2015)
36. L. Xu, S. Li, W. Zhou, Z. Kang, Q. Zhang, M. Kamran, J. Xu, D. Liang, C. Wang, Z. Hou, p62/SQSTM1 enhances breast cancer stem-like properties by stabilizing MYC mRNA. Oncogene **36**, 304–317

(2017)

37. S.D. Soysal, S. Muenst, T. Barbie, T. Fleming, F. Gao, G. Spizzo, D. Oertli, C.T. Viehl, E.C. Obermann, W.E. Gillanders, EpCAM expression varies significantly and is differentially associated with prognosis in the luminal B HER2+, basal-like, and HER2 intrinsic subtypes of breast cancer. Br. J. Cancer **108**, 1480–1487 (2013)
38. C.-W. Lin, M.-Y. Liao, W.-W. Lin, Y.-P. Wang, T.-Y. Lu, H.-C. Wu, Epithelial cell adhesion molecule regulates tumor initiation and tumorigenesis via activating reprogramming factors and epithelial-mesenchymal transition gene expression in colon cancer. J. Biol. Chem. **287**, 39449–39459 (2012)
39. E.L. Gelardi, G. Colombo, F. Picarazzi, D.M. Ferraris, A. Mangione, G. Petrarolo, E. Aronica, M. Rizzi, M. Mori, C. La Motta, A selective competitive inhibitor of aldehyde dehydrogenase 1A3 hinders cancer cell growth, invasiveness and stemness in vitro. Cancers (Basel) **13**, 356 (2021)
40. M. Wienken, A. Dickmanns, A. Nemajerova, D. Kramer, Z. Najafova, M. Weiss, O. Karpiuk, M. Kassem, Y. Zhang, G. Lozano, MDM2 associates with polycomb repressor complex 2 and enhances stemness-promoting chromatin modifications independent of p53. Mol. Cell. **61**, 68–83 (2016)
41. J. Todoric, L. Antonucci, G. Di Caro, N. Li, X. Wu, N.K. Lytle, D. Dhar, S. Banerjee, J.B. Fagman, C.D. Browne, Stress-activated NRF2-MDM2 cascade controls neoplastic progression in pancreas. Cancer Cell. 32, 824–839. e828 (2017)
42. B. Das, B. Pal, R. Bhuyan, H. Li, A. Sarma, S. Gayan, J. Talukdar, S. Sandhya, S. Bhuyan, G. Gogoi, MYC regulates the HIF2α stemness pathway via Nanog and Sox2 to maintain self-renewal in cancer stem cells versus non-stem cancer cells. Cancer Res. **79**, 4015–4025 (2019)
43. V. Damiano, P. Spessotto, G. Vanin, T. Perin, R. Maestro, M. Santarosa, The autophagy machinery contributes to E-cadherin turnover in breast cancer. Frontiers in cell and developmental biology 545 (2020)
44. S.-S. Li, L.-Z. Xu, W. Zhou, S. Yao, C.-L. Wang, J.-L. Xia, H.-F. Wang, M. Kamran, X.-Y. Xue, L. Dong, p62/SQSTM1 interacts with vimentin to enhance breast cancer metastasis. Carcinogenesis **38**, 1092–1103 (2017)
45. C. Gilles, M. Polette, M. Mestdagt, B. Nawrocki-Raby, P. Ruggeri, P. Birembaut, J.-M. Foidart, Transactivation of vimentin by β-catenin in human breast cancer cells. Cancer Res. **63**, 2658–2664 (2003)
46. L. Qiang, Y.-Y. He, Autophagy deficiency stabilizes TWIST1 to promote epithelial-mesenchymal transition. Autophagy **10**, 1864–1865 (2014)
47. X. Sun, Y. Liu, Activation of the Wnt/β-catenin signaling pathway may contribute to cervical cancer pathogenesis via upregulation of Twist. Oncol. Lett. **14**, 4841–4844 (2017)
48. M. Xing, P. Li, X. Wang, J. Li, J. Shi, J. Qin, X. Zhang, Y. Ma, G. Francia, J.-Y. Zhang, Overexpression of p62/IMP2 can promote cell migration in hepatocellular carcinoma via activation of the Wnt/β-catenin pathway. Cancers (Basel) **12**, 7 (2019)
49. C. Dai, A.K. Tiwari, C.-P. Wu, X. Su, S.-R. Wang, D. Liu, C.R. Ashby, Y. Huang, R.W. Robey, Y.-j. Liang, Lapatinib (Tykerb, GW572016) reverses multidrug resistance in cancer cells by inhibiting the activity

of ATP-binding cassette subfamily B member 1 and G member 2. Cancer Res. **68**, 7905–7914 (2008)

50. S. Corrêa, R. Binato, B. Du Rocher, M.T. Castelo-Branco, L. Pizzatti, E. Abdelhay, Wnt/β-catenin pathway regulates ABCB1 transcription in chronic myeloid leukemia. BMC Cancer **12**, 1–11 (2012)
51. B.R. Topacio, E. Zatulovskiy, S. Cristea, S. Xie, C.S. Tambo, S.M. Rubin, J. Sage, M. Kõivomägi, J.M. Skotheim, Cyclin D-Cdk4, 6 drives cell-cycle progression via the retinoblastoma protein's C-terminal helix. Mol. Cell. 74, 758–770. e754 (2019)
52. O. Tetsu, F. McCormick, β-Catenin regulates expression of cyclin D1 in colon carcinoma cells. Nature **398**, 422–426 (1999)
53. J.-L. Qi, J.-R. He, C.-B. Liu, S.-M. Jin, X. Yang, H.-M. Bai, Y.-B. Ma, *SQSTM1/p62 regulate breast cancer progression and metastasis by inducing cell cycle arrest and regulating immune cell infiltration* (Genes & Diseases, 2021)
54. T.M. Puvirajesinghe, F. Bertucci, A. Jain, P. Scerbo, E. Belotti, S. Audebert, M. Sebbagh, M. Lopez, A. Brech, P. Finetti, Identification of p62/SQSTM1 as a component of non-canonical Wnt VANGL2–JNK signalling in breast cancer. Nat. Commun. **7**, 1–15 (2016)
55. A. Schwob, E. Teruel, L. Dubuisson, F. Lormières, P. Verlhac, Y.P. Abudu, J. Gauthier, M. Naoumenko, F.-M. Cloarec-Ung, M. Faure, SQSTM-1/p62 potentiates HTLV-1 Tax-mediated NF-κB activation through its ubiquitin binding function. Sci. Rep. **9**, 1–17 (2019)
56. I. Joung, H.J. Kim, Y.K. Kwon, p62 modulates Akt activity via association with PKCζ in neuronal survival and differentiation. Biochem. Biophys. Res. Commun. **334**, 654–660 (2005)
57. M.A. Fragoso, A.K. Patel, R.E. Nakamura, H. Yi, K. Surapaneni, A.S. Hackam, The Wnt/β-catenin pathway cross-talks with STAT3 signaling to regulate survival of retinal pigment epithelium cells. (2012)
58. B. Davidson, C.G. Tropé, R. Reich, Epithelial–mesenchymal transition in ovarian carcinoma. Front. Oncol. **2**, 33 (2012)
59. C. Pérez-Plasencia, E. López-Urrutia, V. García-Castillo, S. Trujano-Camacho, C. López-Camarillo, A.D. Campos-Parra, Interplay between autophagy and wnt/β-catenin signaling in cancer: therapeutic potential through drug repositioning. Front. Oncol. **10**, 1037 (2020)
60. V.I. Korolchuk, A. Mansilla, F.M. Menzies, D.C. Rubinsztein, Autophagy inhibition compromises degradation of ubiquitin-proteasome pathway substrates. Mol. Cell. **33**, 517–527 (2009)

Scheme

Scheme 1 is available in Supplementary Files section.

Figures

Figure 1

Bee swarm plot of mRNA expression (a) SQSTM1 and (b) β-catenin according to the nature of tissue. Protein expression of (c) SQSTM1 and (d) β-catenin according to the type of breast cancer. Representative immunoblots showing expression of SQSTM1 and β-catenin in (e) MDA-MB-231 and (h) MDA-MB-468 cell extracts, following 48 h of treatment. β-actin serves as a loading control. (f), (g) and (i), (j) are graphical representations of the fold change of SQSTM1 and β-catenin in MDA-MB-231 and MDA-MB-468, respectively. (k) and (l) are pseudo-plot representation of CD44/CD24 population in MDA-MB-231 and MDA-MB-468, respectively.

Figure 2

(a) Assessment of colony formation ability performed in MDA-MB-468. (b) Evaluation of alteration of sphere formation ability following treatment in MDA-MB-468. (c) and (d) is the graphical representation of alteration of colony formation and sphere formation ability in MDA-MB-468. (e), (g) and (f), (h) are the graphical representation of alteration of gene expression following treatment in MDA-MB-231 and MDA-MB-468, respectively. Representative immunoblots showing expression of c-MYC in (i) MDA-MB-231 and (j) MDA-MB-468 cell extracts. β-actin serves as a loading control. (k), (l) is the graphical representation of fold change of c-MYC in MDA-MB-231 and MDA-MB-468, respectively.

Figure 3

Confocal images of MDA-MB-468 monolayer cultures immune-stained with anti-β-catenin antibody visualized by Alexa Flour-488. Actin cytoskeleton was stained with Phalloidin-555. Nuclei were stained with DAPI. Cells were treated with individual inhibitors/ siRNA for 48 h. Scale bar represents 20 μM.

Figure 4

Graphical representation of changes in gene expression levels following treatment with inhibitor/siRNA as quantified by qRT-PCR analysis. (a), (c) and (e) show gene expression levels obtained from MDA-MB-231 monolayer cultures. (b), (d) and (f) show gene expression levels obtained from MDA-MB-468 monolayer cultures. Representative immunoblots showing expression of E-Cadherin in (g) MDA-MB-231 and (i) MDA-MB-468 cell extracts. β-actin serves as a loading control. (h) and (j) are the graphical

representation of fold change of E-Cadherin in MDA-MB-231 and MDA-MB-468, respectively. (k) and (l) are representative histograms depicting alteration of expression of vimentin as obtained by immuno-flow-cytometry in MDA-MB-231 and MDA-MB-468 respectively. All experiments were performed for a time period of 48 h.

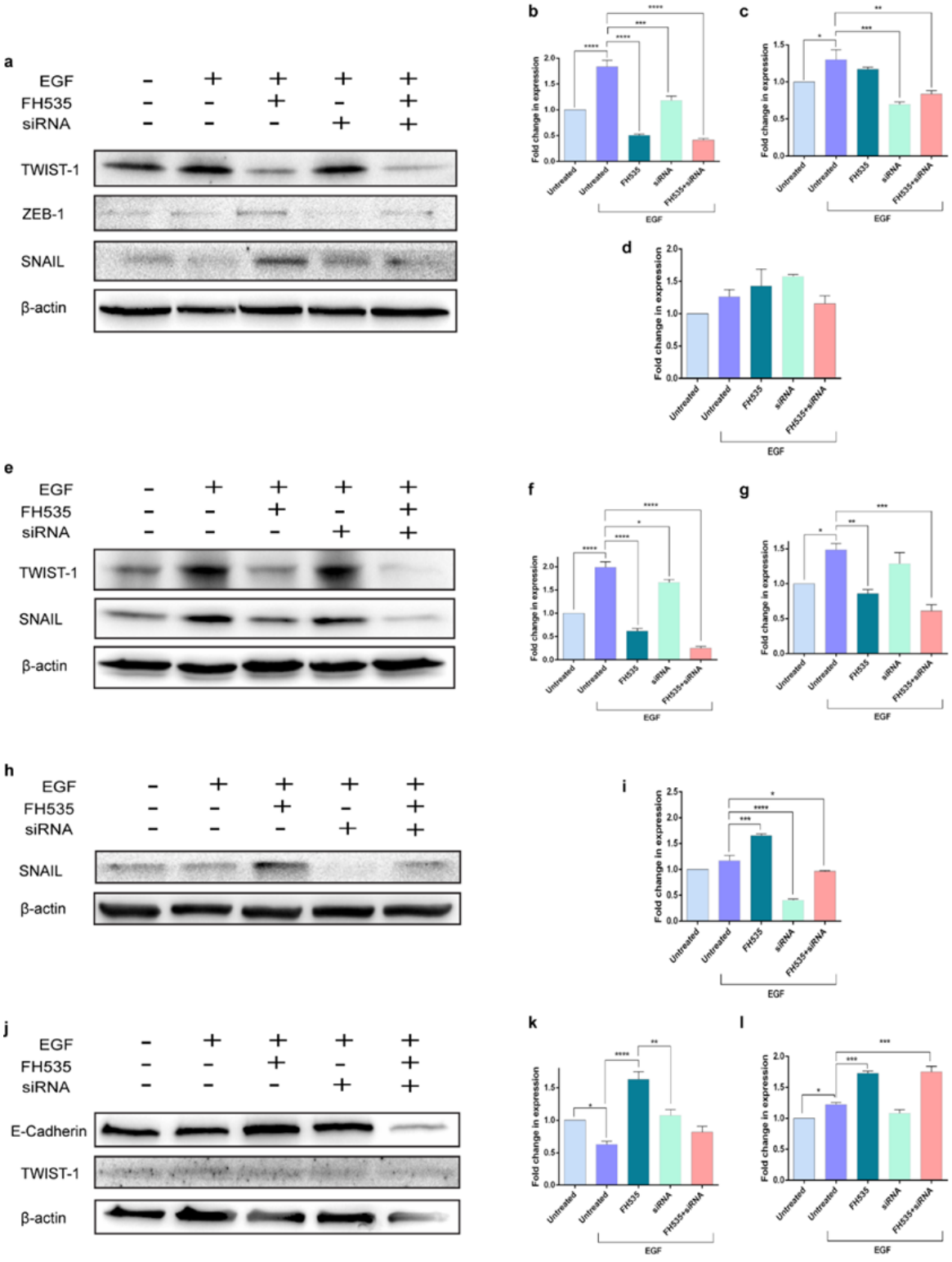

Figure 5

Representative immunoblots showing expression of EMT transcription factors in (a) MDA-MB-231 and (e) MDA-MB-468 monolayer culture cell extracts. β-actin serves as a loading control. (b), (c) and (d) are the graphical representation of fold change of TWIST1, ZEB1 and SNAIL in MDA-MB-231 monolayer culture. (f), and (g) are the graphical representation of fold change of TWIST1 and SNAIL in MDA-MB-468 monolayer culture. (h) and (j) refer to representative immunoblots showing expression of EMT transcription factors in MDA-MB-231 and MDA-MB-468 spheroid cell extracts. β-actin serves as a loading control. (i) is the graphical representation of fold change of SNAIL in MDA-MB-231 spheroid. (k) and (l) are the graphical representation of fold change of E-cadherin and TWIST1 in MDA-MB-468 spheroid.

Figure 6

Confocal images of MDA-MB-231 monolayer cultures immune-stained with anti-vimentin antibody visualized by Alexa Flour-488. Actin cytoskeleton was stained with Phalloidin-555. Nuclei were stained with DAPI. Cells were treated with individual inhibitors/ siRNA for 48 h. Scale bar represents 20 μM.

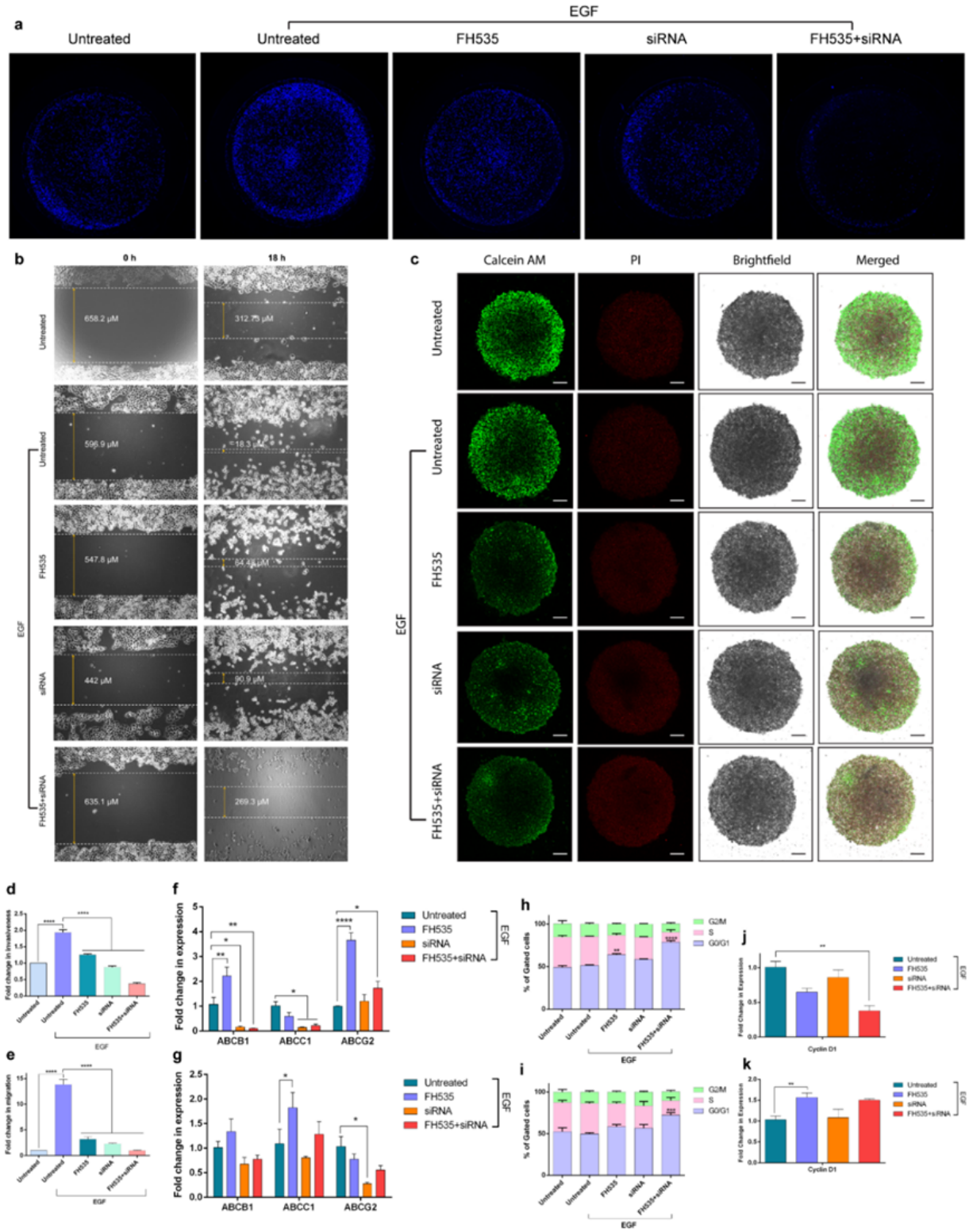

Figure 7

(a) Boyden-chamber invasion assays of MDA-MB-231 monolayer cultures. (b) Scratch wound-healing assays of MDA-MB-468 monolayer cultures. (c) Live-dead cell visualization of MDA-MB-468 spheroids using calcein-AM/propidium iodide (PI) dual staining. Green fluorescence by calcein-AM refers to live cells, whereas red fluorescence by PI refers to dead cells. (d) Graphical representation of changes in invasiveness following inhibitor/siRNA treatment and their combination with respect to untreated

samples. (e) Graphical representation of changes in wound healing capacity following inhibitor/siRNA treatment and their combination with respect to untreated samples. (f) and (g) qRT-PCR analysis of ABC transporters in MDA-MB-231 and MDA-MB-468 following 48 h of treatment. Evaluation of cell cycle profile of (h) MDA-MB-231 and (i) MDA-MB-468. Gene expression graph of Cyclin-D1 of (j) MDA-MB-231 and (k) MDA-MB-468.

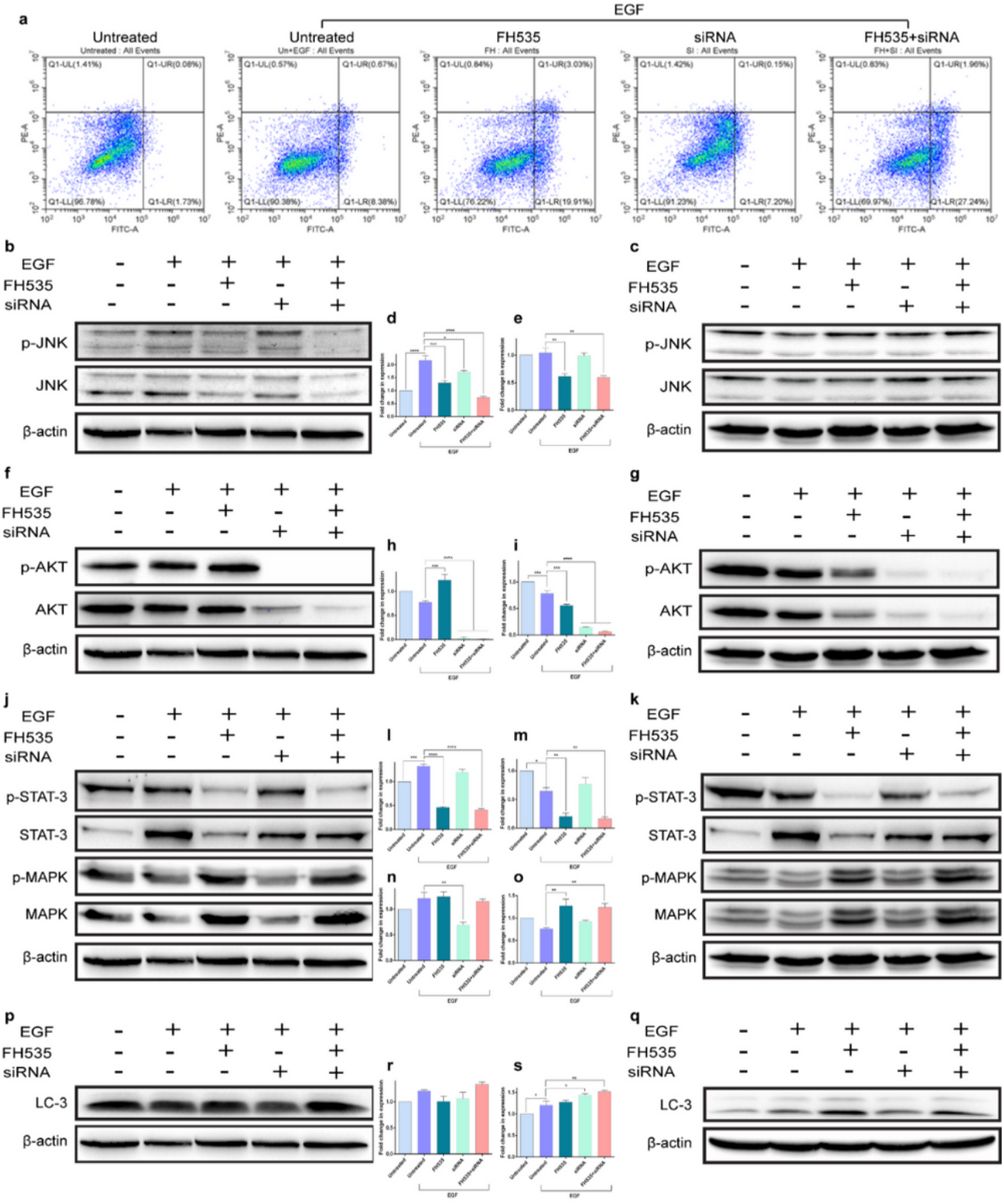

Figure 8

(a) Flow cytometric analysis of apoptotic populations probed by annexin-V-FITC PI assay following treatment in MDA-MB-231 monolayer culture. Representative immunoblots showing expression of (b), (c) p-JNK/JNK and (f), (g) p-AKT/AKT in MDA-MB-231 and MDA-MB-468 cell extracts, respectively. β-actin serves as a loading control. (d), (e) and (h), (i) is the graphical representation of fold change of p-JNK and p-AKT in MDA-MB-231 and MDA-MB-468, respectively. (j) and (k) are immunoblots representing p-STAT-3/STAT-3 and p-MAPK/MAPK in MDA-MB-231 and MDA-MB-468, respectively. (l), (m) and (n), (o) are the graphical representation of fold change of p-STAT-3 and p-MAPK in MDA-MB-231 and MDA-MB-468, respectively. (p) and (q) represent immunoblots of LC-3 from MDA-MB-231 and MDA-MB-468, respectively. (r) and (s) are the graphical representation of fold change of LC-3-II/LC-3-I ratio in MDA-MB-231 and MDA-MB-468, respectively. All the treatments are done for a period of 48 h.

Supplementary Files

This is a list of supplementary files associated with this preprint. Click to download.

- SupportingInformation.docx
- Scheme1.png